Measurement of Electrostatic Potentials above Oriented Single Photosynthetic Reaction Centers

Ida Lee,[†,‡] James W. Lee,[†] Audria Stubna,[†,§] and Elias Greenbaum*[,†]

Chemical Technology Division, Oak Ridge National Laboratory, Oak Ridge, Tennessee 37831-6194, and Department of Electrical Engineering, The University of Tennessee, Knoxville, Tennessee 37996

Received: November 18, 1999; In Final Form: January 21, 2000

Photosystem I (PS I) reaction centers are nanometer-size robust supramolecular structures that can be isolated and purified from green plants. Using the technique of Kelvin force probe microscopy, we report here the first measurement of exogenous photovoltages generated from single PS I reaction centers in a heterostructure composed of PS I, organosulfur molecules, and atomically flat gold. Illumination of the reaction centers was achieved with a diode laser at $\lambda = 670$ nm. Data sets consisting of 22 individual PS Is measured entirely under laser illumination, 12 PS Is measured entirely in darkness, and four PS Is in which the light−dark transition occurred in midscan of a single PS I were obtained. The average values of the light minus dark voltages relative to the substrate for the four PS Is were -1.13 ± 0.14 and -1.20 ± 0.19 V at diametrical peripheries and -0.97 ± 0.04 V at the center. Under illumination, the potentials of the central region of the PS Is were typically more positive than the periphery by 6−9 *kT*, where *kT* is the Boltzmann energy at room temperature. These energies suggest a possible mechanism whereby negatively charged ferredoxin, the soluble electron carrier from PS I to the Calvin−Benson cycle, is anchored and positioned at the reducing end of PS I for electron transfer. The results are placed in context with the prior experimental literature on the structure of the reducing end of PS I.

1. Introduction

Photosynthesis is initiated by vectorial photochemical charge separation. In green plants, photons are captured with high quantum efficiency by two specialized reaction centers, photosystems I and II (PS I and PS II). Photon capture triggers rapid charge separation and the conversion of light energy into an electric voltage across the nanometer-scale reaction centers. The PS I primary electron donor, also known as P700, is a chlorophyll dimer that triggers a photon-induced charge separation. Within PS I, F_A and F_B are the iron sulfur centers that receive electrons from P700 via the intermediate electron carriers A_0, A_1, and F_X. Major structural proteins, PsaA and PsaB, span the membrane to form a scaffold that positions and orients electron donor and acceptor molecules for high quantum efficiency charge separation. Additional protein subunits, PsaC, D, etc., complete the entire PS I reaction center. A schematic illustration of a modern molecular view of the PS I reaction center is presented in Figure 1a.

We have extracted, purified, and contacted PS Is with metallic platinum and anchored them to a metal surface without denaturation.[1,2] Moreover, we have found that PS I reaction centers can be self-assembled and oriented on organosulfur-modified gold substrates and are stable nanometer diodes.[3,4] They possess sufficient functional stability for laboratory experiments and are stable under long-term storage (>4 months). In this Letter, we report the first direct measurement of photovoltages generated by a single PS I, using the technique of Kelvin force probe microscopy (KFM) in the heterostructure composed of PS I, 2-mercaptoethanol, and atomically flat gold. In addition, our measurement of the presence of a local potential minimum at the approximate center of the PS I reaction center may provide insight into the mechanism of electron transfer from F_{AB}[5] to ferredoxin, the stroma-soluble electron relay that carries reducing equivalents to the enzymes of the Calvin−Benson cycle. (According to Golbeck's recent argument, the likely point of electron departure from PS I is F_B[6].) We discuss our results in terms of the recent detailed experiments of Klukas et al.[5] on an improved model of the stromal subunits PsaC, PsaD, and PsaE of PS I.

KFM is a powerful tool that can be used to investigate the local electric potential distribution of semiconductor devices[7,8] and biological samples[9] with nanometer-scale lateral resolution. The technique is based on elementary electrostatic interactions between tip and sample. Like electrostatic force deflections of the well-known gold-leaf electroscope, no current flows in this voltage-measuring technique. As described by Jacobs et al.,[10] the force between tip and sample is given by $F_z = {}^1/_2\, dC/dz(\Delta\Phi)^2$, where C is the capacitance, $\Delta\Phi$ the potential between tip and sample, and z the vertical coordinate. An electric potential image with minimum cross-talk is obtained by sequential measurement of topography and potential using the lift-mode technique.[10] Correlation between the actual surface potential distribution and measured quantities is given by $\Phi_{DC} = [C'_{1t}\Phi_1 + C'_{2t}\Phi_2]/[C'_{1t} + C'_{2t}]$, where Φ_{DC} is the measured potential, Φ_1 is the substrate (nonlocal) potential, Φ_2 is the actual surface potential of an object on the surface (local potential), and the values of C'_{1t} and C'_{2t} depend on the geometry of the KFM tip and the diameter of the object that is imaged. Optimum performance of the KFM is achieved when the sum of local electrostatic interactions predominates over the sum of nonlocal

* Corresponding author. E-mail: greenbaume@ornl.gov.
† Oak Ridge National Laboratory.
‡ The University of Tennessee.
§ Oak Ridge National Laboratory Energy Research Undergraduate Laboratory Fellow.

10.1021/jp994119+ CCC: $19.00
Published on Web 02/26/2000

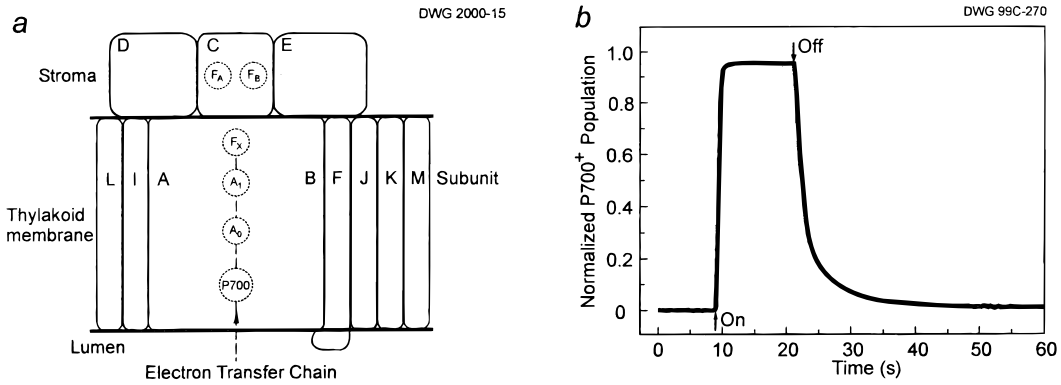

Figure 1. (a) Schematic illustration of the molecular architecture of photosystem I. Redrawn from ref 22. (b) Kinetic profile of $P700^+$ steady-state formation and reduction. The actinic light was turned on and off at the indicated times. The light-induced steady-state formation of $P700^+$ in this figure is the functional biochemical equivalent of the light-induced single-molecule steady-state voltage measured in Figures 3 and 4.

interactions.[11] This is favored by a long slender tip with a slightly blunt apex. In this case, the measured potential will be approximately equal to the actual potential.[11]

2. Experimental Section

PS I reaction center/core antenna complexes containing about 40 chlorophylls per photoactive P700 (PS I-40) were isolated from spinach thylakoids using detergent (Triton X-100) solubilization and hydroxylapatite column purification.[12] PS I was eluted in a buffer which contained 0.2 M phosphate pH 7.0 and 0.05% Triton X-100. The characteristics of the PS I reaction centers were confirmed by absorption spectroscopy (maxima at 440 and 672 nm) and by P700 oxidation kinetic spectroscopy in the presence of 20 mM sodium ascorbate and 0.5 mM methyl viologen, illustrated in Figure 1b. P700 oxidation measurements were performed with a Walz spectrometer that measured the kinetic profile of the light-induced differential absorption between 810 and 860 nm. In the presence of sodium ascorbate, the reduction kinetics of $P700^+$ are biphasic: 24 s^{-1} for reduction by F_{AB}^- and 0.1 s^{-1} by ascorbate.

Since PS I-40 was isolated with the nonionic detergent Triton X-100, it most likely contains subunits PsaC and PsaD that donate electrons to ferredoxin in natural photosynthesis. A detailed study[12] of the photooxidation and reduction kinetics of $P700^+$ demonstrated that PS I-40 has a "fast" $P700^+$ reduction component (24 s^{-1}), corresponding to the recombination of $P700^+$ and F_{AB}^-.[13] Also, since it is known that PsaC contains F_{AB}^- and is closely associated with PsaD, the presence of F_{AB}^- indicates the presence of PsaC and PsaD in PS I-40. Therefore, it is likely that the structure of the reducing end of PS I-40 is similar to that of PS I in vivo.

Flat single-crystal gold substrates (Au{111}) were prepared by evaporation of 120 nm gold films onto freshly cleaved mica heated to a temperature of 300−400 °C. Gold surfaces were chemically modified by a 30 s immersion in a 10 mM solution of 2-mercaptoethanol, rinsed thoroughly in Nanopure water, and air-dried by ultrapure nitrogen (0.2 ppm of O_2, 1.9 ppm of H_2O, undetectable total hydrocarbons). This technique of directed self-assembly for PS I has been previously reported.[4] The treated surfaces were incubated at 3.7 °C for 14 h in a buffered PS I solution, washed by Nanopure distilled water, and dried with ultrapure nitrogen prior to the KFM measurement. Measurement was performed in ultrapure helium at relative humidity less than 0.01%.

In situ calibration of the Kelvin force microscope was achieved with specially prepared structures in which gold was sputtered on ultraflat cover-glass slides. Dc step voltages provided by a constant voltage source were correlated with the electric potential image map of the structures obtained with KFM. The calibration data indicated a minimum detection limit of 10 mV with a 1 mV standard deviation.

A modified Nanoscope IIIa (Digital Instruments) was used to study PS I topography and light-induced electric potentials. Tapping mode atomic force microscopy (AFM) surface topography of a single line was first scanned (Figure 2a) and recorded (Figure 2b) followed immediately by a second scan of the line for electric potential measurement at a set height of 40 nm away from the sample surface, using the built-in lift-mode feature illustrated in Figure 2, c and d. The lift-mode scan tracked the previously stored surface topographic scan. AFM topography and the corresponding KFM electric potential were recorded in sequential scans at a scan rate of 1 Hz; 265 lines were scanned in two segments over the sample area to form two-dimensional images. A diode laser (670 nm) was switched on for the first segment of the scan and off for the second.

3. Results and Discussion

As previously reported,[4] 70−80% of PS Is on 2-mercaptoethanol-modified gold substrates are oriented primarily with the electron acceptor side up (adjacent to the tip), and the P700 donor side down (adjacent to the 2-mercaptoethanol-modified gold surface). Control experiments (data not shown) with the light on and off indicated that topography of the PS I reaction centers was the same in light and darkness. The topographic image size of PS I recorded in Figure 3a is 45.7 ± 7.4 nm, a value larger than the actual size. This well-known broadening effect[14] is caused by the relatively blunt KFM tip which, while exaggerating feature size, improves the accuracy of electric potential measurement. The KFM image in Figure 3b demonstrates a clear light-induced PS I electric potential reversal from positive voltage to negative upon illumination during the second segment of the scan. Under illumination, the electric potential on the reducing side of PS I develops a negative voltage following electron capture, whereas in the dark, the potential is positive. This result is consistent with the well-known vectorial photophysics occurring in the PS I reaction center in the photosynthetic membrane and with our previous discovery of the orientation of PS I on 2-mercaptoethanol-modified gold surfaces.[4] It is also consistent with the known physical−chemical properties of the reaction centers. The PS I core reaction center retains 40 chlorophyll molecules with an optical cross section of ≈1 $Å^2$ per chlorophyll.[15] On the basis of absolute measurements of laser power and spot size, photon flux from the diode

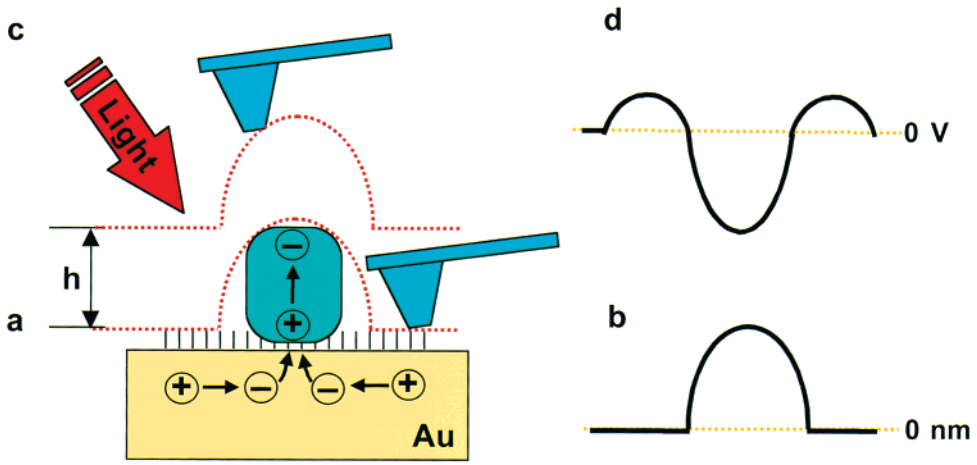

Figure 2. Schematic illustration of the technique used for photovoltage measurement of single PS I reaction centers. Dual measurements employed (a) tapping mode AFM for topographic imaging and (c) lift-mode KFM for voltage imaging. (b) AFM trace; (d) KFM trace under illumination. The peripheral local positive potential under illumination was created by the movement of electrons toward the $P700^+$. See text for additional details.

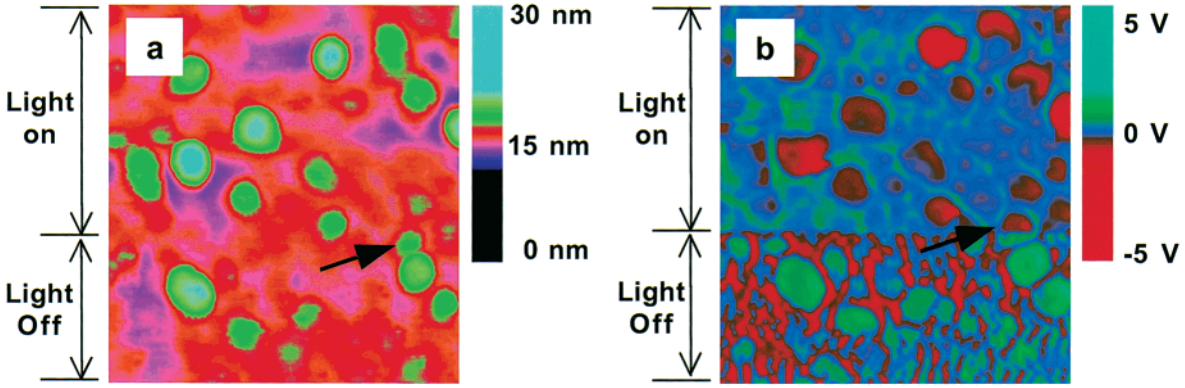

Figure 3. (a) Topographic and (b) electric potential image maps of the same set of isolated and oriented PS I reaction centers on a 2-mercaptoethanol-modified gold surface. Although clearly evident, the one-to-one image correspondence is not perfect since, as previously reported,[4] the degree of orientation is 70−80%. Part b demonstrates a clear light-induced PS I electric potential reversal from positive voltage to negative upon illumination. Under illumination, the electric potentials of PS I acceptors F_A and F_B develop a negative voltage following electron capture, whereas in the dark, the potential is positive. The scanning directions for each raster of the constructed images were from left to right and top to bottom.

laser light source is 9.6×10^3 photons s^{-1} $Å^2$. Therefore, the rate of photon excitation of a PS I reaction center, $\approx 3.8 \times 10^5$ s^{-1}, is at least 10^4 times greater than the rate of $P700^+$ reduction by F_{AB}^- (24 s^{-1}). Under these conditions of illumination, the PS I reaction center is biased in the negative state.

During the normal course of KFM image scans, the diode laser was turned on and off in two sequential segments. Therefore, virtually all the PS I reaction centers were imaged either entirely in light or entirely in darkness. However, for a small sample of PS Is, the diode laser was turned off in midscan. The arrow of Figure 3a points to one such reaction center and is shown enlarged in Figure 4a. Just below this reaction center is another PS I imaged in complete darkness. (Figure 4d is an example of a PS I reaction center that was nearly equally "bisected" by the horizontal light/dark scan.) The electric potential voltage vs distance profile along the cross-sectional axis of the lower (Figure 4a) PS I imaged with light off is shown in Figure 4b. The vertical arrows in Figure 4b indicate three selected voltage points of this reaction center: the two extremities and the center. Typically, as illustrated in Figure 4b, the central voltage was always lower than the extremities and may be suggestive of structural features of PS I. The average potentials of 12 different PS Is (light off) at these three locations are 0.77 ± 0.14, 0.62 ± 0.08, and 0.99 ± 0.20 V, as shown in Table 1 under the "dark" column. This measurement demonstrates that the ground-state reducing end of PS I has a positive surface charge relative to the base under these experimental conditions. Electrons in different materials have different chemical binding energies. When two dissimilar materials, such as PS I and derivatized gold, are in physical contact, local interfacial electron density redistributes itself from the material with the smaller work function to the material with the higher work function. This charge migration is consistent with the equilibrium electrostatic forces observed in Figure 4b. Similar measurements were performed with the light on (Figure 4c). These reveal negative potentials with values at the center slightly more positive than those at the extremities. The average potentials of 22 PS Is (light-on) at these three locations are -0.47 ± 0.26, -0.41 ± 0.24, and -0.59 ± 0.26 V, as shown in Table 1 under the "light" column. Higher standard deviations of PS I electric potential measurements were observed in the light compared to darkness. This is most likely due to the statistical variance of electron−hole recombination following photon absorption. That is to say, since further electron transfer is blocked in isolated PS I reaction centers, it returns to $P700^+$ by charge recombination with F_{AB}^- and interaction with electrons from the gold substrate periphery that migrate toward the center of positive charge created by $P700^+$ (Figure 2).

As mentioned above, several PS I reaction centers were fortuitously "bisected" with light during the scanning process. This enabled measurement of electric potential difference on the same PS I reaction center between light on and light off.

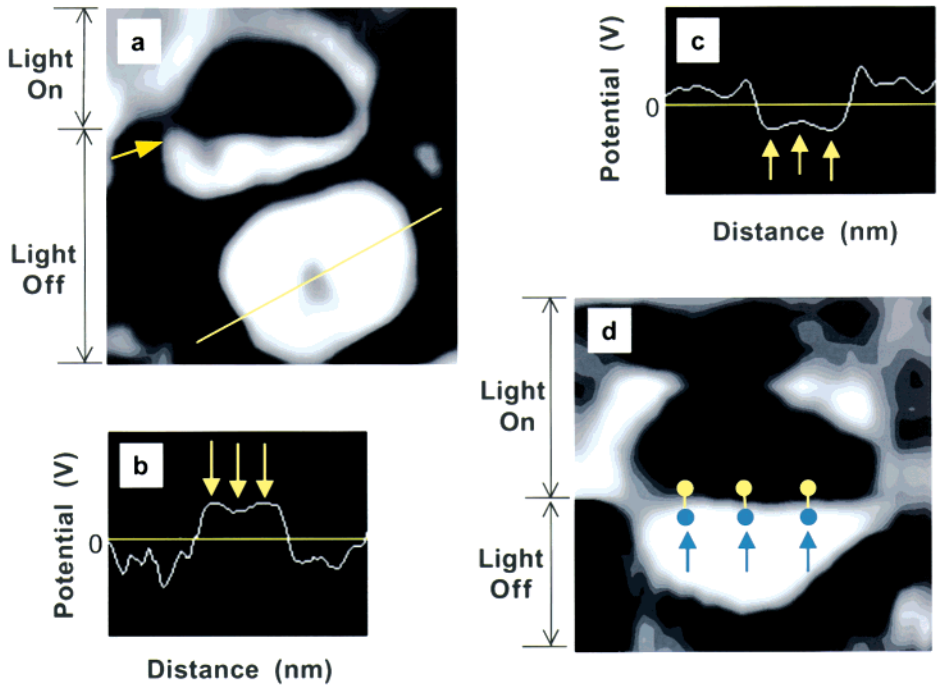

Figure 4. Detailed views of KFM images of individual PS I reaction centers and corresponding cross-sectional voltage−distance profiles. (a) View of selected area of Figure 3b. Of the two PS I reaction centers (RCs), the lower RC was imaged entirely in darkness, whereas the upper RC was imaged mostly in light. Note the abrupt change in electric potential for the upper RC as the diode laser was switched off in midscan at the indicated location. (b) Light off voltage−distance profile along the indicated cross-sectional axis. (c) Light on voltage−distance profile. (d) A single PS I RC was "bisected" in midscan by switching the diode laser off. Voltage difference measurements in light and darkness, indicated by the proximal dots, were taken at the peripheries and the center.

TABLE 1: PS I Photovoltage Topography: Summary of Three Types of Measurements

	dark (A)	light (B)	(B − A)[a]	light−dark[b]
periphery 1 (V)	0.77 ± 0.14	−0.47 ± 0.26	−1.24 ± 0.29	−1.13 ± 0.14
center (V)	0.62 ± 0.08	−0.41 ± 0.24	−1.03 ± 0.25	−0.97 ± 0.04
periphery 2 (V)	0.99 ± 0.20	−0.59 ± 0.26	−1.58 ± 0.32	−1.20 ± 0.19
no. of PS Is averaged	12	22		4

[a] Calculated difference between columns B and A. [b]On the same PS I.

As shown in Figure 4d, the potential difference between two points, one in light and the other in darkness, is connected by a vertical line. Six representative data points were selected for comparison. The average light on/off potential differences of 4 PS Is (of which one is illustrated in Figure 4d) at these locations are −1.13 ± 0.14, −0.97 ± 0.04, and −1.20 ± 0.19 V, as shown in Table 1 under the "light−dark" column.

Significant experiments on electron microscopy,[16,17] cross-linking,[18,19] and X-ray crystallography[20−22] have led to progressively more detailed models of the PS I stromal ridge, demonstrating that the PsaC, PsaD, and PsaE subunits are in close proximity to each other. More recently, Klukas et al. have presented the first structural model of PsaD.[5] The model indicates that PsaD partly covers PsaC stromally in a clasplike manner and approaches and interacts with PsaE. The three small subunits form a stromal ridge that extends ≈3 nm beyond the membrane integral region. In addition, the three small subunits form a wide cavity, which serves as the docking site for ferredoxin as first suggested by Fromme et al.[23] Viewed in the context of this rich prior literature on the structure of the reducing end of PS I (especially Figure 3a of ref 5), we feel that the central local minimum of the PS I reaction center of the present study may be significant. Even for an ionic species bearing a single electrostatic charge e^-, the energy of interaction of the potential well exceeds the Boltzmann energy, 0.025 eV. The abrupt light-induced reversal of peripheral local minimum to central local minimum may indicate the peripheral docking and light-induced movement of ferredoxin to the center of PS I for electron acceptance from the F_{AB}^- site. Put another way, we interpret the functional clasplike action of the three small subunits of Klukas et al.[5] in terms of light-induced electrostatic potential energy surfaces creating a local binding minimum for ferredoxin that is justified in terms of the energy of interaction, at least several multiples of *kT*.

This analysis is also consistent with the properties of the biomimetic photosynthetic system in which metallic platinum precipitated at the point of electron emergence from PS I catalyzes the evolution of molecular hydrogen.[24,25] In this case the precipitation reaction is

$$[PtCl_6]^{2-} + 4e^- \rightarrow Pt\downarrow + 6Cl^-$$

in which PS I itself is the source of electrons. PS I-driven hydrogen evolution will not occur from chloroplast membranes unless it is contacted with metallic platinum. Therefore, negatively charged $[PtCl_6]^{2-}$, like negatively charged ferredoxin, may be moved to the proper location by the light-induced local potential minimum created at the center of PS I. Metallic platinum is precipitated at precisely the point of electron emergence and catalyzes the evolution of molecular hydrogen. This interpretation is also supported by the fact that the positively charged ionic platinum species, $[Pt(NH_3)_4]^{2+}$, will

not produce a hydrogen-evolving material even when precipitated on photosynthetic membranes.[24] This ionic species evidently does not find the right location at the stroma-membrane interface.

4. Conclusion

The data presented here demonstrate the first direct measurement of photovoltages from single PS I reaction centers. The polarity and magnitude of the light-induced voltage are consistent with the known structural and energetic features of PS I. In addition, the discovery of a local central potential minimum, corresponding to energy interactions exceeding the Boltzmann energy kT at room temperature, suggests a docking and orientation mechanism for the transfer of electrons from the F_{AB}^- site to ferredoxin.

Acknowledgment. We thank M. L. Simpson, M. Guillorn, D. H. Lowndes, and G. Eres for comments and discussions, and L. Wagner for secretarial support. This research was supported by the U.S. Department of Energy, the ORNL Laboratory Director's R&D Fund, the Defense Advanced Research Projects Agency, and the Research Institute for Innovative Technology for the Earth. Oak Ridge National Laboratory is managed by Lockheed Martin Energy Research Corp. for the U.S. Department of Energy under contract DE-AC05-96OR22464.

References and Notes

(1) Lee, J. W.; Lee, I.; Laible, P. D.; Owens, T. G.; Greenbaum, E. *Biophys. J.* **1995**, *69*, 652−659.

(2) Lee, J. W.; Lee, I.; Greenbaum, E. *Biosens. Bioelectron*. **1996**, *11*, 375−387.

(3) Lee, I.; Lee, J. W.; Warmack, R. J.; Allison, D. P.; Greenbaum, E. *Proc. Natl. Acad. Sci. U.S.A.* **1995**, *92*, 1965−1969.

(4) Lee, I.; Lee, J. W.; Greenbaum, E. *Phys. Rev. Lett.* **1997**, *79*, 3294−3297.

(5) Klukas, O.; Schubert, W.-D.; Jordan, P.; Krauss, N.; Fromme, P.; Witt, H. T.; Saenger, W. *J. Biol. Chem.* **1999**, *274*, 7351−7360.

(6) Golbeck, J. H. *Photosynth. Res.* **1999**, *61*, 107−144.

(7) Vatel, O.; Tanimoto, M. *J. Appl. Phys.* **1995**, *77*, 2358−2362.

(8) Arakawa, M.; Kishimoto, S.; Mizutani, T. *Jpn. J. Appl. Phys., Part 1* **1997**, *36*, 1826−1829.

(9) Fujihira, M.; Kawate, H. *J. Vac. Sci. Technol. B* **1994**, *12*, 1604−1608.

(10) Jacobs, H. O.; Knapp, H. F.; Muller, S.; Stemmer, A. *Ultramicroscopy* **1997**, *69*, 39−49.

(11) Jacobs, H. O.; Leuchtmann, P.; Homan, O. J.; Stemmer, A. *J. Appl. Phys.* **1998**, *84*, 1168−1173.

(12) Lee, J. W. Ph.D. Dissertation, Cornell University, Ithaca, NY, 1993.

(13) Golbeck, J. H.; Bryant, D. A. *Curr. Top. Bioenerget.* **1991**, *16*, 83−177.

(14) Vesenka, J.; Miller, R.; Henderson, D. *Rev. Sci. Instrum.* **1994**, *65*, 2249−2251.

(15) Kauzmann, W. *Quantum Chemistry*; Academic Press: New York, 1957; p 583.

(16) Böttcher, B.; Gräber, P.; Boekema, E. J. *Biochim. Biophys. Acta* **1992**, *100*, 125−136.

(17) Kruip, J.; Chitnis, P. R.; Lagoutte, G.; Rögner, M.; Boekema, E. J. *J. Biol. Chem.* **1997**, *272*, 17061−17069.

(18) Jansson, S.; Andersen, B.; Scheller, H. V. *Plant Physiol.* **1996**, *112*, 409−420.

(19) Armbrust, T. S.; Chitnis, P. R.; Guikema, J. A. *Plant Physiol.* **1996**, *111*, 1307−1312.

(20) Krauss, N.; Hinrichs, W.; Witt, I.; Fromme, P.; Pritzkow, W.; Dauter, Z.; Betzel, C.; Wilson, K. S.; Witt, H. T.; Saenger, W. *Nature* **1993**, *361*, 326−331.

(21) Krauss, N.; Schubert, W.-D.; Klukas, O.; Fromme, P.; Witt, H. T.; Saenger, W. *Nat. Struct. Biol.* **1996**, *3*, 965−973.

(22) Schubert, W.-D.; Klukas, O.; Krauss, N.; Saenger, W.; Fromme, P.; Witt, H. T. *J. Mol. Biol.* **1997**, *272*, 741−769.

(23) Fromme, P.; Schubert, W.-D.; Krauss, N. *Biochim. Biophys. Acta* **1994**, *1187*, 99−105.

(24) Greenbaum, E. *Science* **1985**, *230*, 1373−1375.

(25) Greenbaum, E. *J. Phys. Chem.* **1988**, *92*, 4571−4574.